Sustainable Cities and Society 104 (2024) 105288

Contents lists available at ScienceDirect

Sustainable Cities and Society

journal homepage: www.elsevier.com/locate/scs

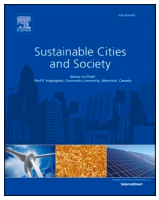

Connected urban green spaces for pluvial flood risk reduction in the Metropolitan area of Milan

Andrea Staccione [a,b,c,*], Arthur Hrast Essenfelder [d], Stefano Bagli [e], Jaroslav Mysiak [a,b]

[a] CMCC Foundation, Euro-Mediterranean Center on Climate Change Edificio Porta dell'Innovazione, Piano 2, Via della Libertà, 12 Marghera, 30175, Venice (VE), Italy
[b] Ca' Foscari University of Venice, Edificio Porta dell'Innovazione - Piano 2, Via della Libertà, 12 Marghera, 30175, Venice (VE), Italy
[c] Institute of Meteorology and Climate Research, Atmospheric Environmental Research (IMK-IFU), Karlsruhe Institute of Technology, Kreuzeckbahnstraße 19, 82467 Garmisch-Partenkirchen, Germany
[d] European Commission, Joint Research Centre (JRC), Via E. Fermi, 2749, 21027 Ispra (VA), Italy
[e] GECOsistema srl, Geographic Environmental Consulting, Unità R&D Suedtirol: via Maso della Pieve/Pfarrhofstr, 60/A, 39100 Bolzano (BZ), Italy; Legal Seat: Piazza Malatesta, 21- 47923 Rimini (RN), Italy

ARTICLE INFO

Keywords:
Green infrastructure
Pluvial flood
Damage
Population exposed
Connectivity
Risk reduction

ABSTRACT

Rethinking cities in a more sustainable and integrated way is a key opportunity for successful climate change adaptation and disaster risk management. Nature-based solutions and green infrastructures can help to safeguard urban nature and biodiversity while providing multiple benefits to reduce climate risks and improve human well-being. Nature-based solutions help to mitigate flood risk by regulating storm-water runoff and peak-flow. This paper investigates the effects of nature-based solutions and green infrastructure networks on pluvial flood risk in the Milan metropolitan area in terms of direct economic damage to buildings and population exposed. Results show that extending the urban green networks by 25 % can potentially halve the pluvial flood damages and reduce the population exposed by 40 %. For all analysed rainfall intensities, damages to buildings and share of population exposed decrease (up to 60 % and 50 % respectively) as green area coverage increases, with slightly higher flood risk reduction for lower-intensity events. The applied methodological framework makes it possible to identify priority-action urban areas and hence inform decision-making processes as for where green solutions are most efficient.

1. Introduction

The Sixth Assessment Report of IPCC (Intergovernmental Panel on Climate Change) identifies cities and urban environments as hotspots of impacts and risks associated with climate change, but it also recognises the important role they can play to fight the climate crisis (IPCC, 2022).

Nowadays, about half of world population is living in cities while in Europe and Italy urban population is even higher (63.5 % and 56 %, respectively) (ISTAT, 2020). Urbanisation is a major cause of fragmentation and degradation of natural ecosystems, potentially exacerbating the economic, social, and environmental impacts of climate change (UNEP and UN-Habitat, 2021). Under future climate conditions, urban areas are likely to be at higher risk of extreme weather events and increased impacts in terms of casualties and economic losses and damages (IPCC, 2022; Spano et al., 2021b).

Hydrological and meteorological hazards (e.g. floods, mass movement and storms) are accountable for the largest economic losses from weather- and climate-related events in Europe (EEA, 2022). Italy is one of the European countries with the highest economic flood risk, with damages exceeding 38 billion Euros over the period 1980-2020 (Mysiak et al., 2022). These impacts are not equally distributed: Lombardy, for instance, is among the regions with the highest economic damages, accounting for the 14 % of national losses in the 2000s (Carrera et al., 2015), and with the highest exposure to flood hazard (Lastoria et al., 2021). In a +2 °C warmer world, the annual flood damages in Italy are expected to exceed 3 billion Euro and to affect almost 40,000 people every year if no adaptation actions are taken (Dottori et al., 2020). Without adaptation actions, Lombardy is expected to suffer economic losses around 140 million Euro/year due to floods in the 2080s (Carrera et al., 2015).

Pluvial flood (i.e. due to rainfall intensity exceeding infiltration capacity) risk is particularly pronounced in urban environments due to the

* Corresponding author.
E-mail address: andrea.staccione@cmcc.it (A. Staccione).

https://doi.org/10.1016/j.scs.2024.105288
Received 6 November 2023; Received in revised form 5 February 2024; Accepted 18 February 2024
Available online 19 February 2024

generally lower permeability of the soil surface in these areas. Indeed, urbanisation and soil sealing contribute to increasing pluvial flood risks due to lower infiltration rates and higher surface runoff values (EEA, 2017).

Rethinking cities in a more sustainable and integrated way offers a key opportunity for climate change adaptation and mitigation. Green and energy-efficient buildings (Cirrincione et al., 2021; Ercolani et al., 2018), sustainable transport systems (Sharifi, 2021; Łukaszkiewicz et al., 2021), and urban green spaces (Misiune and Kazys, 2022; EEA, 2021; Pamukcu-Albers et al., 2021) can provide a viable contribution to climate- and weather-related risk reduction. These so-called nature--based solutions (NBS), i.e. actions inspired and supported by nature that simultaneously provide environmental, social and economic benefits, can help building resilience to climate change (EC, 2015).

In this working-with-nature framework, green infrastructures (GI) play a prominent role, especially in the urban environment. GI are defined as "*strategically planned network of natural and semi-natural areas with other environmental features designed and managed to deliver a wide range of ecosystem services*" (EC, 2013a). GI provide multiple ecosystem services that contribute to reducing climate risks and improving human well-being, such as carbon sequestration, food and water provision, flood and climate regulation, recreational and social opportunities. Protecting urban nature and biodiversity is a key function of GI. They act on flood regulation by increasing the water retention or infiltration capacity of the soil (EC, 2013b). In urban environments, GI such as urban parks, rain gardens, green alleys, green roofs, and permeable pavements can increase water retention capacity. This helps to reduce stormwater runoff and peak flows, which in turn limits the economic and social losses and damage (EEA, 2017, 2021).

In this context, Du et al. (2019) investigated the role of concave green land in mitigating urban flooding in central Shanghai, China, by integrating urban flood simulation, scenario analysis, and mitigation assessment, concluding that GI can not only mitigate direct runoff and inundation, but also reduce population exposure and enhance community resilience. Similarly, La Rosa and Pappalardo (2020) explored the role of sustainable urban drainage systems (in particular, green roofs) in reducing the intensity of pluvial flood hazard in densely populated catchments in Sicily, Italy, concluding that this type of nature-based solution can not only reduce the intensity of flood hazard but also the overall pluvial flood risk measured in terms of population affected. In turn, Andrés-Doménech et al. (2018) monitored and evaluated the performance of green roofs at building and city scales under in Benaguasil, Valencia, Spain, concluding that green roofs can potentially reduce flood risks at the building and city scales even in relatively dry climates such as the Mediterranean. Other examples of recent advancements in flood regulation by means of GI include the assessment of the effectiveness of planning and building regulations in coping with urban flooding under precipitation uncertainty (Piyumi et al., 2021), a multi-dimensional urban flood risk assessment supported by stakeholders' perceptions for the ranking/prioritization of districts (Ekmekcioğlu et al., 2022), an innovative multi-attribute and non-stationary decision model for managing flood risks in urban areas under climatic and demographic changes (da Silva et al., 2022), and the development of an urban flood vulnerability index based on an interlinked social-ecological-technological systems vulnerability framework (Chang et al., 2021).

The positive impacts of GI in reducing urban flood risk are well addressed in the literature. However, there is a significant knowledge gap in terms of peer-reviewed and empirically sound studies that quantitatively measure the performance of these solutions (Sudmeier--Rieux et al., 2021). Particularly, how GI distribution and connectivity across a city influence their effectiveness is barely considered in the context of disaster risk reduction and climate adaptation. To enhance the expected benefits, including flood regulation capacity, GI should be also strategically connected across the space (Staccione et al., 2022a). Building a green urban network and improve connectivity and proximity of green areas is fundamental to maintain healthy and well-functioning ecosystems that can support multiple ecological functions and delivery the expected services (Mitchell et al., 2015; Monteiro et al., 2020). This is also in line with the emerging "15-minutes City" approach for a more sustainable and resilient urban development, already applied in several cities as Paris, Barcelona and Melbourne, that aim to include all the daily services for citizens in a walking or cycling radius of around 15 minutes (Moreno et al., 2021).

This paper contributes to address this gap, including the network perspective in flood risk analysis. Combining pluvial flood hazard modelling and GI network design, the paper aims to evaluate the implementation and impact of GI measures in the context of disaster risk reduction, considering the unique characteristics of the urban study areas. The study defines implementation scenarios for GI in the city of Milan, Italy, considering new and diverse criteria, such us flood risk, connectivity, accessibility to green spaces, and feasibility of conversion. Based on these criteria, the study proposes tailored scenarios for green conversion, enabling decision-makers to prioritize interventions based on their specific development and adaptation goals. This approach allows for the assessment of expected impacts and helps in identifying suitable solutions for achieving desired outcomes, providing an overview and mapping of possibilities. GI effectiveness is reported in terms of direct economic damages to building and population exposed.

The paper presents the case study of Milan in Section 2. The method section is structured in three parts: (i) analysis of the current green network (Section 3.1), (ii) definition of scenarios for green network improvement (Section 3.2), and (iii) the assessment of green network scenarios effects on pluvial flood risk (Section 3.3). Results are presented in Section 4, followed by a discussion of the main findings and implications of the study (Section 5), and conclusions (Section 6).

2. Case study: the metropolitan area of Milan

The Metropolitan City of Milan is the administrative centre of Lombardy Region (Fig. 1). It is the second-largest city in Italy, highly developed with strong economic and industrial sectors, and densely populated, being home to 3.3 million residents.

Milan is located in the Padan Plain, an alluvial plain generated by the Po River and its major tributaries, and is crossed by Lambro, Seveso and Olona rivers. Due to its orographic and hydrographic conformation, the city is exposed to a significant flood risk, enough to be one of the Italian cities with the highest number of disaster events in Italy, especially linked to urban floods (Spano et al., 2021a). The 4 % of municipal land resulted to be subjected to High Probability Flood Hazard (HPH) and

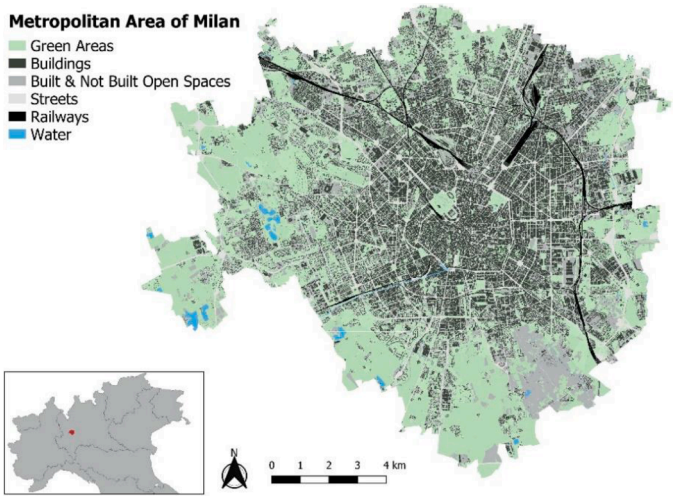

Fig. 1. Metropolitan Area of Milan. The map shows the main classes derived from ESM (Ferri et al., 2017), particularly the green areas used in the analysis.

10.9 % of land subjected to Low Probability Flood Hazard (LPH); with 1.5 % of population living in HPH areas and 9 % of population living in LHP areas (Lastoria et al., 2021). In the period 2010-2020, the city experienced 29 disaster events linked to intense precipitation, causing 20 river floods, 19 days of stop for transportation systems, several electricity black-out events, with severe economic and social impacts (Zanchini et al., 2020). In the past decades, the climate in Milan has been characterised by increasing temperature, increasing number of tropical nights and decreasing of total precipitation (ISTAT, 2022). The climate projections for 2100 are following the same trends of temperature and precipitation, but with increasing frequency and intensity of extreme rain events (IPCC, 2021; Myhre et al., 2019; Fischer and Knutti, 2016; Spano et al., 2021a). This will increase, at the same time, the risk of urban pluvial floods and heat waves (Spano et al., 2021a).

Milan has established a series of plans and strategies to address climate change. Urban green spaces and infrastructures are among the key actions identified. Today, the green areas cover about 13.8 % of municipal territory, mainly urban parks, gardens and historical green areas and green urban design elements (ISTAT, 2022). There are about 37 trees for 100 inhabitants, corresponding to 18 m^2 per inhabitant of green area (Laurenti and Bono, 2020). Important are the larger parks surrounding the city (such as Parco Nord, Parco Agricolo Sud, Parco della Media Valle del Lambro), which have aesthetic and ecological characteristics relevant to the city and act as elements of connection with the regional ecological network (Comune di Milano, 2019a). As part of the Covenant of Mayor for Climate and Energy, C40 Cities Climate and Leadership Group and 100 Resilient Cities Network initiatives (C40 Cities - Milan, 2024; Resilient Cities Network - Milan, 2024), the city aims to become more sustainable and resilient through urban green regeneration. The Urban Development Plan for 2030 (Comune di Milano, 2019b) and the Air and Climate Plan (Comune di Milano, 2020) address heat waves and flood risks through a strong implementation of NBS to increase water infiltration and limit the soil sealing. To this end, the city is investing in several project to plant 3 million of trees and increase the canopy coverage of 5 % by 2030, support the installation of green roofs and walls in private and commercial buildings, reopen and greening the channel network, create permeable surface, green areas, vegetated rails and bus stops.

3. Methods

Fig. 2 shows the methodological framework underpinning this study. The analysis follows three main phases that are described in detail in the next sections. The analysis of the existing urban green infrastructure network (Fig. 2.1, Section 3.1) aims to assess the current coverage, distribution and connection of green areas. This will help identify areas that require interventions, such as green conversion and increased green accessibility, or areas that must be preserved. The existing GI network is then used as baseline to define different network improvement scenarios (Fig. 2.2, Section 3.2) aimed at reducing flood risk by introducing new green areas and elements. Finally, the study assesses the effects of different scenarios (baseline and green conversion scenarios) on pluvial flood risk using a pluvial flood hazard mapping model and a risk-centred damage function (Fig. 2.3, Section 3.3).

3.1. Urban green infrastructure network analysis

The analysis is based on the framework developed in Staccione et al. (2022b). The first step is to define the green elements to be included in the network. To achieve this, all the existing green spaces identified in the European Settlement Map (resolution 2.5 m – Fig. 1), reclassified on a regular grid of 100 m, have been used (Ferri et al., 2017). Only cells with more than 25 % of green coverage are included in the network. The resulting grid is then used as input to perform the morphological spatial pattern analysis, identifying GI network elements as core areas (network nodes) and connectors (network links) (Vogt et al., 2009; Soille and Vogt, 2009). This allows for investigation of network connectivity using a landscape connectivity index. Landscape connectivity indices are valuable for analysing network structure from a spatial perspective, considering the location, quantity and characteristics of landscape elements (Staccione et al., 2022a). The Integrate Index of Connectivity (IIC) has been selected for this purpose (Pascual-Hortal and Saura, 2006). The IIC is a simple binary graph-based index that analyses the presence or absence of connections. It informs about the connectivity status of the entire network with low data requirements. The IIC increases from 0 to 1 as the connectivity increases. The IIC has the ability to assess and rank the contribution and importance of each core area to the overall network connectivity, detecting the critical areas that require conservation or

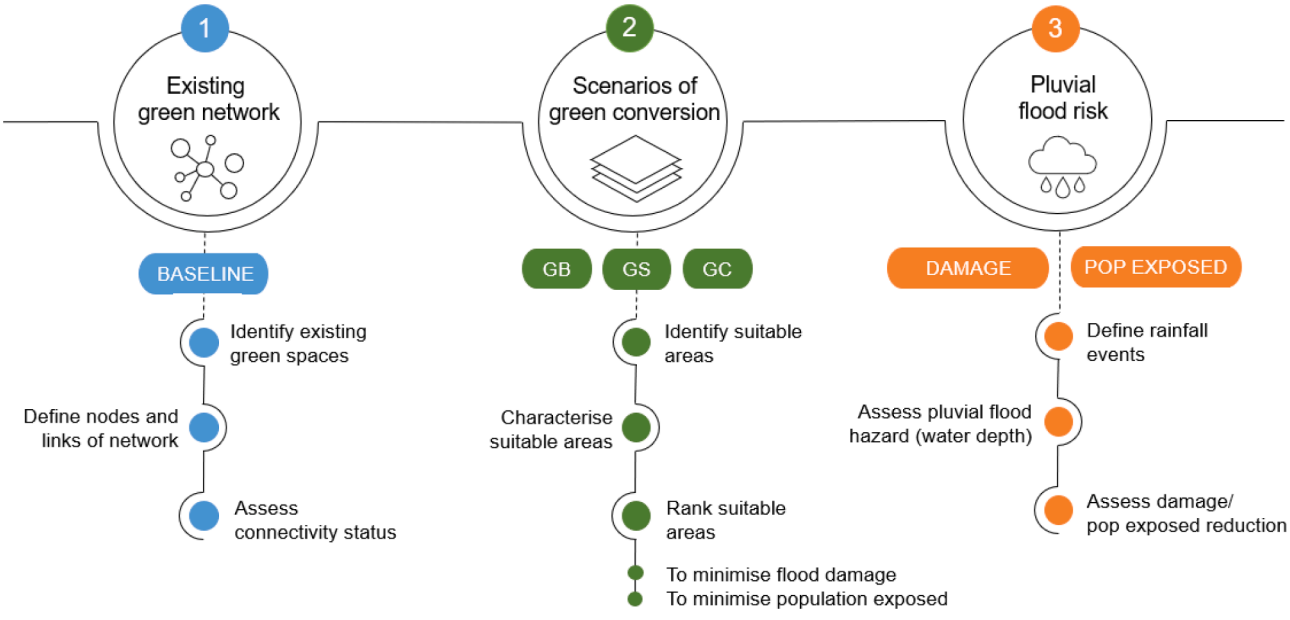

Fig. 2. Methodological framework of the analysis. The overall process consists of three main phases that aim to 1) assess the current status of urban green network, 2) develop scenarios of green network improvement, and 3) assess the impact of each scenario in reducing pluvial flood risk, in terms of direct damage to buildings and population exposed.

intervention (Pascual-Hortal and Saura, 2006; Saura and Rubio, 2010). The formulas and details for IIC are provided in the Annex.

3.2. Urban green infrastructure improvement scenarios

Three scenarios of green conversion have been hypothesised based on the current green coverage: (i) Green Buildings (GB), which involves the establishment of new green roofs; (ii) Green Spaces (GS), which entails converting open, ground spaces to additional green spaces; and (iii) Green City (GC), which combines both GB and GS. Each scenario for green conversion investigates four different incremental percentages of green conversion: 25 %, 50 %, 75 %, and 100 % of all potential green areas.

Within scenarios, the areas to be converted to green have been identified according to a set of criteria, that help to define potentially relevant areas in terms of connectivity and potential reduction of pluvial flood risks. In line with the goal and plan of Milan's city administration to improve proximity and accessibility to different services and green spaces (Comune di Milano, 2019b), a first criterion used is the walking distance (5 to 10 minutes) from existing green areas. This allows to select areas that can enhance the connectivity of exiting green network and can play a role in a wider climate adaptation strategy. The walking distance criteria determine the suitable cells that could guarantee accessibility to a green area every 5-10 minutes of walk, encompassing both existing and potential areas. Then, for the scope of the analysis, the identified areas were characterised by: (i) the cumulative flood direct damages to buildings, obtained from Essenfelder et al. (2022), measured as the existing potential damage per cell in RP100 events (Fig. 3a); (ii) the current residential population per cell, obtained from Schiavina et al. (2019) and SISI (2021) (Fig. 3b); (iii) the share of existing open spaces that can be turned to green per cell, obtained from Ferri et al. (2017) (Fig. 3c); (iv) the share of roofs that are suitable to green roofs installation per cell, obtained from Comune di Milano (2016) (Fig. 3d) and (v) the impact of potential conversion to green roofs per cell, defined as a function of sealed areas in the surrounding area (i.e. the higher the imperviousness of the area, the higher the expected impact) and obtained from Comune di Milano (2016) (Fig. 3e). These criteria allow to characterise each suitable cell in terms of potential flood risk (measured as the direct cumulative economic damage and population exposed) and potential land use conversion (measured as the percentage of the cell that can be converted to green). All the above-mentioned criteria were then normalised by feature-scaling, with resulting values ranging between 0 and 1. Feature-scaling normalisation has been applied as it provides feature-independent results in the same range for all the considered criteria, avoiding any penalty or bias towards one criterion over the other.

Finally, the criteria have been combined to rank the suitable areas based on their contribution to reducing flood risk. Two different rankings have been computed for two different prioritisation goals: (i) minimising flood damages and (ii) minimising population exposed. The ranking identifies priority-areas for the total percentages of green conversion in each scenario by selecting the top-ranked areas up to the total area defined for the green conversion scenario (e.g. 25 %, 50 %, etc.). This is done first by computing the scenario with 100 % green conversion, and then by ordering the resulting prioritisation goals metrics and selecting the cells from the highest values to the lowest. The ranking analysis assumed an equally-weighted product function approach between the criteria (i.e. by means of a simple product aggregation method to rank the areas where a higher potential for minimising direct damages to buildings and to population exposed to floods exist). A product function approach is chosen as it allows for detecting and exacerbating highly undesirable situations when a single criterion might perform the worst (e.g. a situation of maximum flood damage or maximum population exposed is highly undesirable, irrespectively on how well any

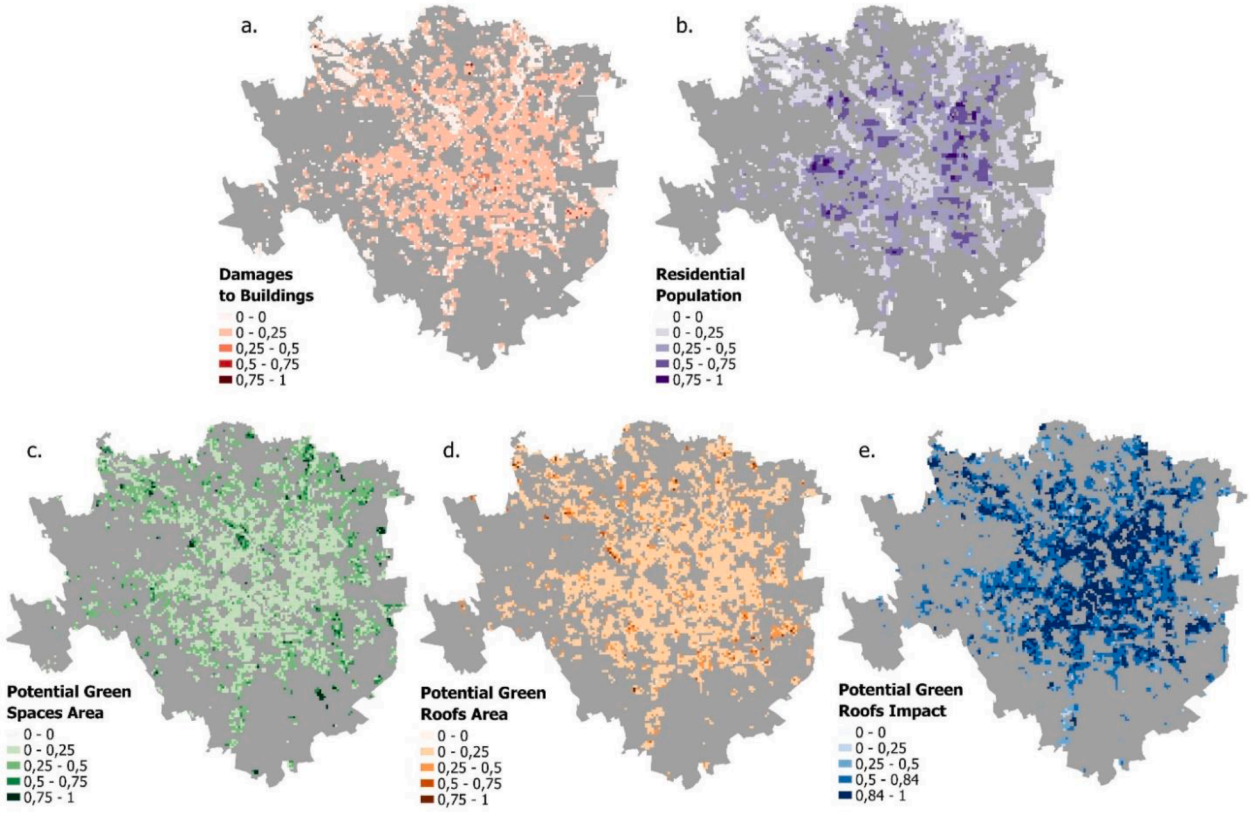

Fig. 3. Characterisation of the suitable areas for green conversion according to the defined evaluation criteria: a) damage to buildings; b) residential population; c) potential green spaces area; d) potential green roofs area; e) potential green roofs impact.

Table 1
Ranking functions for each scenario. Cells have been ranked from higher to lower values.

	Minimise Flood Damage	Minimise Population Exposed
Green Buildings	Damage × Green Roof Area × Green Roof Impact	Population × Green Roof Area × Green Roof Impact
Green Spaces	Damage × Green Space Area	Population × Green Space Area
Green City	Damage × Green Roof Area × Green Roof Impact × Green Space Area	Population × Green Roof Area × Green Roof Impact × Green Space Area

other criteria behaves; moreover, by considering an equally-weighted approach, a greening scenario leading to either maximum flood damage or maximum population exposed is never selected as a desirable solution). The equally-weighted approach is motivated by the fact that no preference is given to a flood damage reduction over population exposure (and vice-versa); here, preferences from a decision-maker could play a role in deciding which criteria could be more relevant, but without having access to such information the adoption of an equally-weighted approach was preferred. The equally-weighted product function approach, while not directly assigning preferences to one criterium over another, is still on itself the result of the combination of the selected criteria by means of a function, thus based on a value judgment on how the index is built and computed. As such, potential users of the here proposed methodology are advised to carefully evaluate the suitable of the index for their specific applications. The equations shown below indicate the generic aggregation functions for flood damage (Eq. 1) and population exposure (Eq. 2).

$$(D)^{\omega_{fd}} \cdot (G_{RA})^{\omega_{gra}} \cdot (G_{RI})^{\omega_{gri}} \cdot (G_{SA})^{\omega_{gsa}} \quad (1)$$

$$(P)^{\omega_{fp}} \cdot (G_{RA})^{\omega_{gra}} \cdot (G_{RI})^{\omega_{gri}} \cdot (G_{SA})^{\omega_{gsa}} \quad (2)$$

Where, for every cell, D is the normalized flood damage reduction potential, P is the normalized population exposure reduction potential, G_{RA} is the normalized green roof area, G_{RI} is the normalized green roof impact, G_{SA} is the normalized green space area, ω_{fd} is the weight parameter for prioritising flood damage reduction, ω_{fp} is the weight parameter for prioritising population exposure reduction, ω_{gra} is the weight parameter for prioritising the conversion of areas to green roofs, ω_{gri} is the weight parameter for prioritising the conversion of areas to green roofs impacts, and ω_{gsa} is the weight parameter for prioritising the conversion of areas to green spaces.

For the design of the different greening scenarios, we consider three different greening scenarios, each focusing on different conversion types to green areas and their respective combination with either potential flood damage reduction D or potential population exposure reduction P. The greening scenarios are: (i) green buildings (G_{RA} and G_{RI}), where ω_{gsa} is set to 0 and all other ω are set to 1; (ii) green space (G_{RA}), where ω_{gra} and ω_{gri} are set to 0 and all other ω are set to 1, and; (iii) green city, where all three green area parameters are accounted for with all ω set to 1. Since we assume an equally-weighted approach for each parameter in a scenario (i.e. all weights ω that are not set to 0 are equal to 1), the definition of the greening scenarios from the aggregation functions shown in Eqs. 1 and 2 are reduced to the simple product of the normalized features considered in each greening scenario, as shown in Table 1.

3.3. Urban green infrastructure assessment

Flood risk is defined based on the definition of risk from the IPCC Special Report on Managing the Risks of Extreme Events and Disasters to Advance Climate Change (SREX) (IPCC, 2012), in which risk is a function of hazard, exposure, and vulnerability. Each greening scenario was used as input for the Safer_RAIN model (Samela et al., 2020) to estimate flood hazard. Safer_RAIN is a static filling and spilling pluvial hazard model which identifies pluvial flood prone areas on the basis of surface depressions that could store precipitation water volumes. The Safer_RAIN model is specifically designed for pluvial flood risk assessment, incorporating various factors such as rainfall intensity, land use, and infiltration rates. The model is powerful to quickly estimate hotspot areas of water accumulation and assess the changes of water depth according to different surface conditions, such as the incorporation of green infrastructure scenarios. For the case study of Milan as explored in this research, a 2 m-resolution elevation model derived from LIDAR data available from the Lombardy Region was used (Regione Lombardia, 2022). The model generates pluvial flood hazard maps over urban areas by accounting for spatially distributed rainfall input and for infiltration processes. Of particular relevance for urban environments and a main limitation of the model, Safer_RAIN is not capable of explicitly accounting for the presence of stormwater drainage network systems. To account for the presence of stormwater drainage network systems in the metropolitan area of Milan, we perform a post-processing of the generated flood maps by assuming a maximum drainage capacity corresponding to a precipitation event associated with a return period as the no-damage baseline. Having no access to the actual design of the stormwater drainage network system of Milan, and acknowledging the fact that assuming a spatially consistent, flawlessly designed and perfectly maintained urban stormwater drainage system with a fixed return period is a source of uncertainty, we consider three different maximum drainage capacity levels: a first of five years (RP 5, shown in details in the Results section) (Skougaard Kaspersen et al., 2017) and also of 10 years (RP 10) and of twenty-five years (RP 25, both shown in details in Annex). Infiltration rate in Safer_RAIN is computed by means of a pixel-based Green–Ampt model, while soil properties are obtained from the European Soil Database v2.0 (Panagos, 2006). A key parameter that connects the potential green coverage of an area and infiltration is the imperviousness of the soil, a parameter that ranges from 0 (impervious) to 1 (completely permeable) (see Samela et al. 2020). The imperviousness at the baseline scenario is derived from the high-resolution layer on imperviousness density data (EEA, 2018). The greening scenarios account for the changes in the potential green area coverage in each cell, which is in turn a function of the share of green roof (GB), open green spaces (GS), or both (GC). The analysis considered

Table 2
Rain events for the metropolitan area of Milan (Essenfelder et al., 2022; CNR-GNDCI, 2001).

Return Period	Hourly rainfall Intensity [mm]
RP 5	33.36
RP 10	38.52
RP 25	45.04
RP 50	49.88
RP 100	54.68

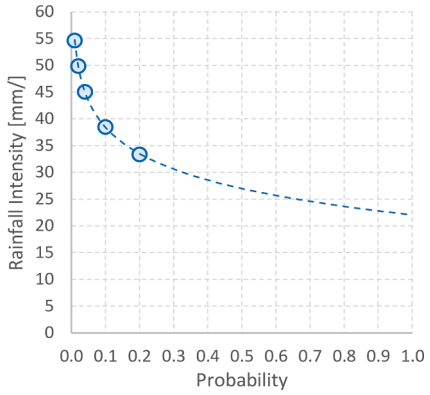

extreme rainfall events of 1 hour with different rain intensities as estimated in Essenfelder et al. (2022) to assess changes in water depth by changing imperviousness in the different scenarios of green conversion. Rainfall intensities are defined in accordance with the estimated depth-frequency values of extreme precipitation events (Table 2).

The flood hazard is defined through the flood extent and water depth outputs obtained from Safer_RAIN (Samela et al., 2020). Exposure is defined by means of built-up environment and population density. Built-up environment is assessed by means of buildings data that have been retrieved from OpenStreetMaps (OSM, 2021), while population density is retrieved from a 100m resolutions dataset named GHS-POP R2019A (Schiavina et al., 2019). Vulnerability is assessed for built-up areas only and is computed by using a direct damage estimation function retrieved from Huizinga et al. (2017) to evaluate the potential reduction of damages to buildings for each scenario, compared to the existing green coverage (baseline). The damage estimation is performed following the work in Essenfelder et al. (2022) and is based on a depth-damage vulnerability function linking the hazard magnitude to the value of exposed assets (Huizinga et al., 2017), while building reconstruction costs are extracted from country-specific cadastral estimates per type of building, i.e. residential, commercial and industrial (EC-Harris, 2010). Damage results are expressed as percentage reduction and Expected Annual Damage (EAD) and computed using the trapezoidal method (Olsen et al., 2015). For each rain event, the expected damage is compared between the current green condition and the potential green coverage scenarios. With regards to population density, lacking access to a specific flood damage function for population in the case study area, the analysis assessed the population exposed six classes of water depth: 0-0.05; 0.05-0.1; 0.1-0.25; 0.25-0.5; 0.5-1; >1 m. For each scenario of green conversion and rain intensity, the population living in the different classes of flooded areas is counted. Results are reported as percentage reduction and Expected Annual Exposed Population (EAPE).

4. Results

4.1. Milan green infrastructure network

The existing GI network in the city of Milan is shown in Fig. 4. The city has a significant presence of green areas, but mainly concentrated in the peripheral zones of the city. Here, the network is well developed and has important core areas supporting the overall connectivity. The inner part of the city, on the other hand, has few or no core green areas, that are disconnected and contribute to a low connectivity value (IIC = 0.1).

4.2. Greening scenarios

Around 6350 suitable cells that could guarantee accessibility to a green area every 5-10 minutes of walk have been identified. These are mainly distributed in inner part of the city, in accordance with the highlighted needs. The top 25 % of potential areas prioritised for minimising the damage and the population exposed in the GC scenarios are reported in Fig. 5. For the full set of scenarios see the Annex. The combination of the criteria produced different ranking of areas according to their contribution to minimize the damage and the population exposed. New green areas result to be distributed throughout the city, potentially acting as green corridors between central and peripheral green areas. They provide a reduction in imperviousness, based on the share of potential new green areas per cell, that is higher in the green city scenarios with respect to the solely green spaces and green buildings conversion. Major improvements are visible in areas closer to existing green spaces.

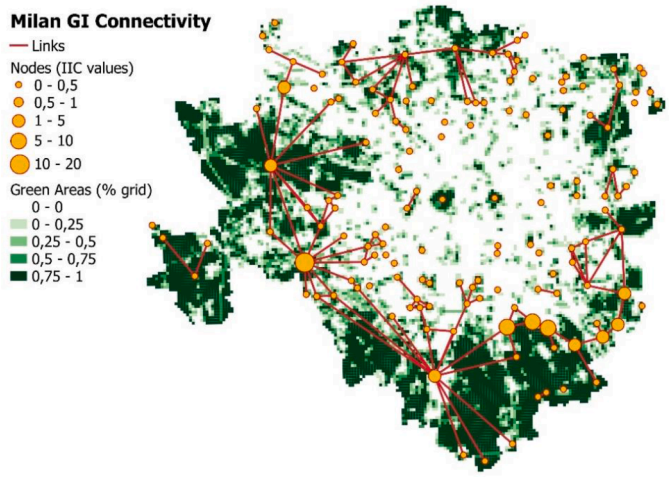

Fig. 4. Existing GI Network in the City of Milan. The lines (connections) and dots (core areas) are the graphical representation of the network. The size of dots indicates the importance of the area to the overall connectivity of the network (IIC values). The green grid represents the ESM green areas reclassified on a grid of 100m. Green shades correspond to the share of green areas in each cell and represent the baseline used in the analysis.

4.3. Green network assessment

As discussed in the methods section, the results shown in this section depicts in full details the main findings when assuming a maximum drainage capacity corresponding to a precipitation event with a return period of five years, while, where appropriate, comparing those results with a maximum drainage capacity of both RP10 and RP25 precipitation events. Readers interested in checking the results under the RP10 and RP25 maximum drainage capacity assumptions are invited to read the Annex.

4.3.1. Damage to buildings

For each scenario of green conversion, a progressive reduction of the expected damage to buildings at the increasing of green coverage is observed (Fig. 6). Generally, results show higher effects in case of lower rain intensities, with similar effects for both the tested configurations, i.e. minimizing the damage to buildings and minimizing the population exposed. The two configurations show some differences at the lower levels of green conversion, being almost equivalent in the 100 % of potential greening, for all the types of conversion. The Green City scenarios lead to higher damage reduction for all rain intensities. For more extreme events (RP100) the percentage reduction of damage is close to 60 % in RP100 (77 % and 100 % when maximum drainage capacity corresponds to RP10, RP25 respectively). Green Spaces scenarios reach a damage reduction of around 35 % in the most extreme scenario (around 45 % and 80 % in RP10 and R25 max. drainage capacity), while Green Buildings scenarios provide the lower impacts for extreme rainfall events of up to 20 % (around 30 % and 50 % in RP10 and R25 max. drainage capacity). Nevertheless, both GS and GB show important damage reduction for lower rain intensities.

The expected annual damage to buildings is significantly reduced. Fig. 7 shows the probability of damage curves referred to the minimization of damage configuration and Table 3 reports a summary of EAD estimated values. At the current conditions, the EAD is around 18.6M€ (8.1M€ and 1.9 M€ for RP10 and RP25 max. drainage capacity). In GC scenarios, the EAD is halved with the 25 % of additional green areas (around 60 % and 80 % reduction in RP10 and RP25 max. drainage capacity). At the same percentage of conversion, the EAD is reduced by a

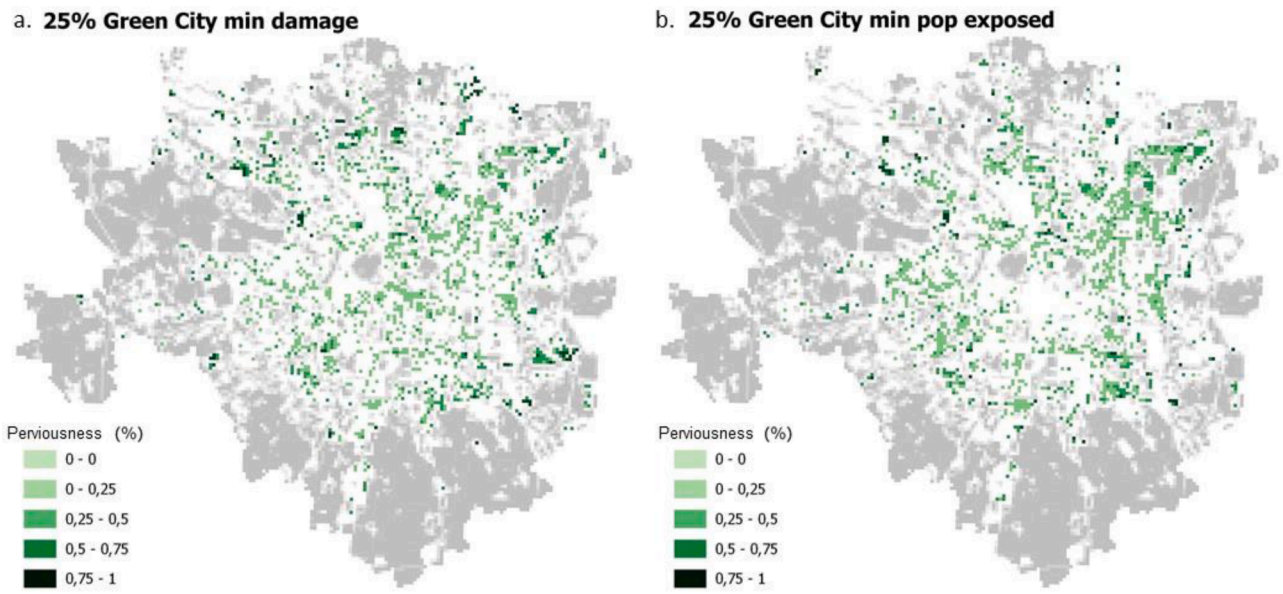

Fig. 5. Examples of green scenarios. Top 25% of green conversion in green city scenario: a) configuration to minimise damage; b) configuration to minimise population exposed. Green shades represent the percentage of green conversion (from 0 to 1, from fully impervious to completely pervious) in each cell. Grey cells represent the existing green network (baseline).

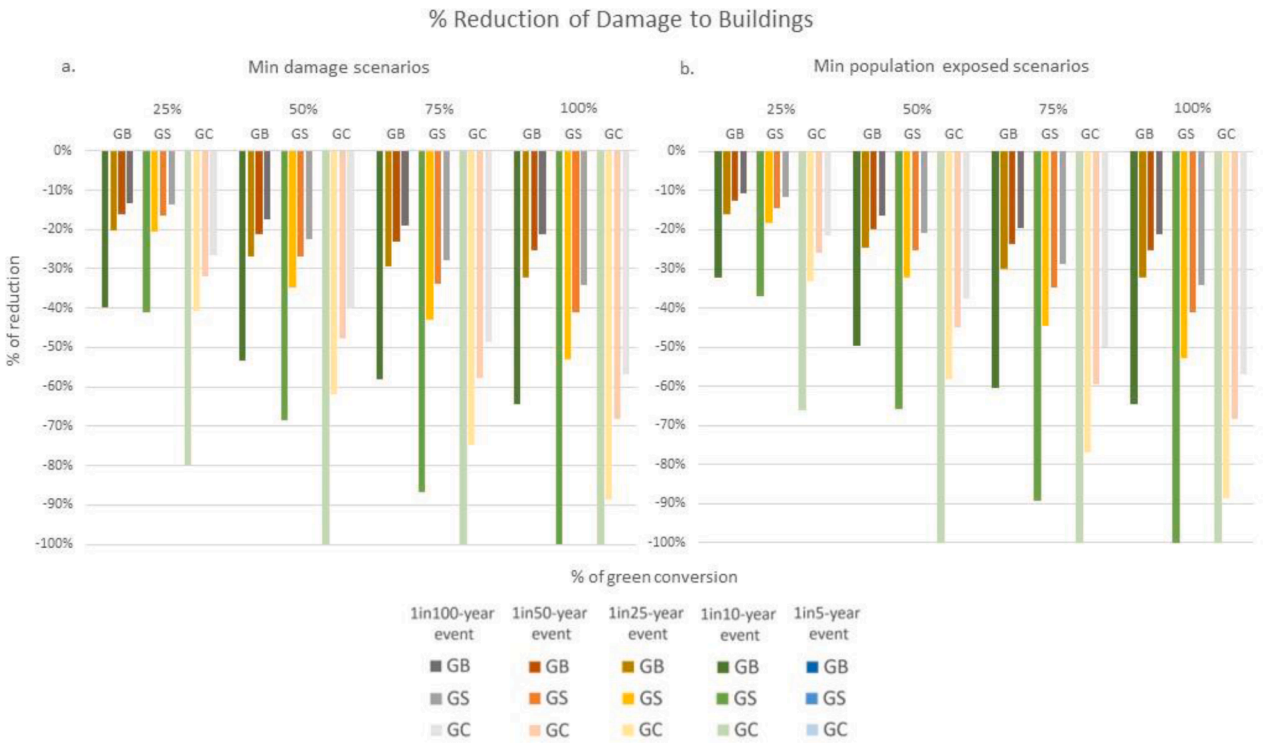

Fig. 6. Percentage reduction of damage to buildings for each scenario of conversion compared to the baseline when assuming a maximum drainage capacity corresponding to a precipitation event of RP5. On the left, a) reduction associated with the minimization of damage scenarios; b) reduction associated with the minimization of population exposed scenarios. The x-axis represents the percentage of green conversion (25% to 100%) for each scenario of conversion (GB, GS, GC), while y-axis reports the percentage reduction of damage to buildings and population exposed.

quarter in GS and in GB (around 30 % and 45 % reduction in RP10 and RP25 max. drainage capacity). Similar values resulted for the minimization of population configuration (in Annex). These results show how the combination of measures, both green roofs and green open areas, better contribute to flood risk reduction by providing major infiltration rates of the soil (as observed in Fig. 5).

4.3.2. *Population exposed*

Results for the population exposed showed similar trends. Fig. 8 reports the results for the population exposed to pluvial floods, showing the total population exposed to water depth >5 cm and that exposed to extreme class of water depth > 100 cm. With the increase of green coverage, less people are generally affected by pluvial floods for all rain intensities. In case of Green City scenarios, the percentage reduction of population exposed ranges from 8 % to 45 % in for water depth > 5 cm

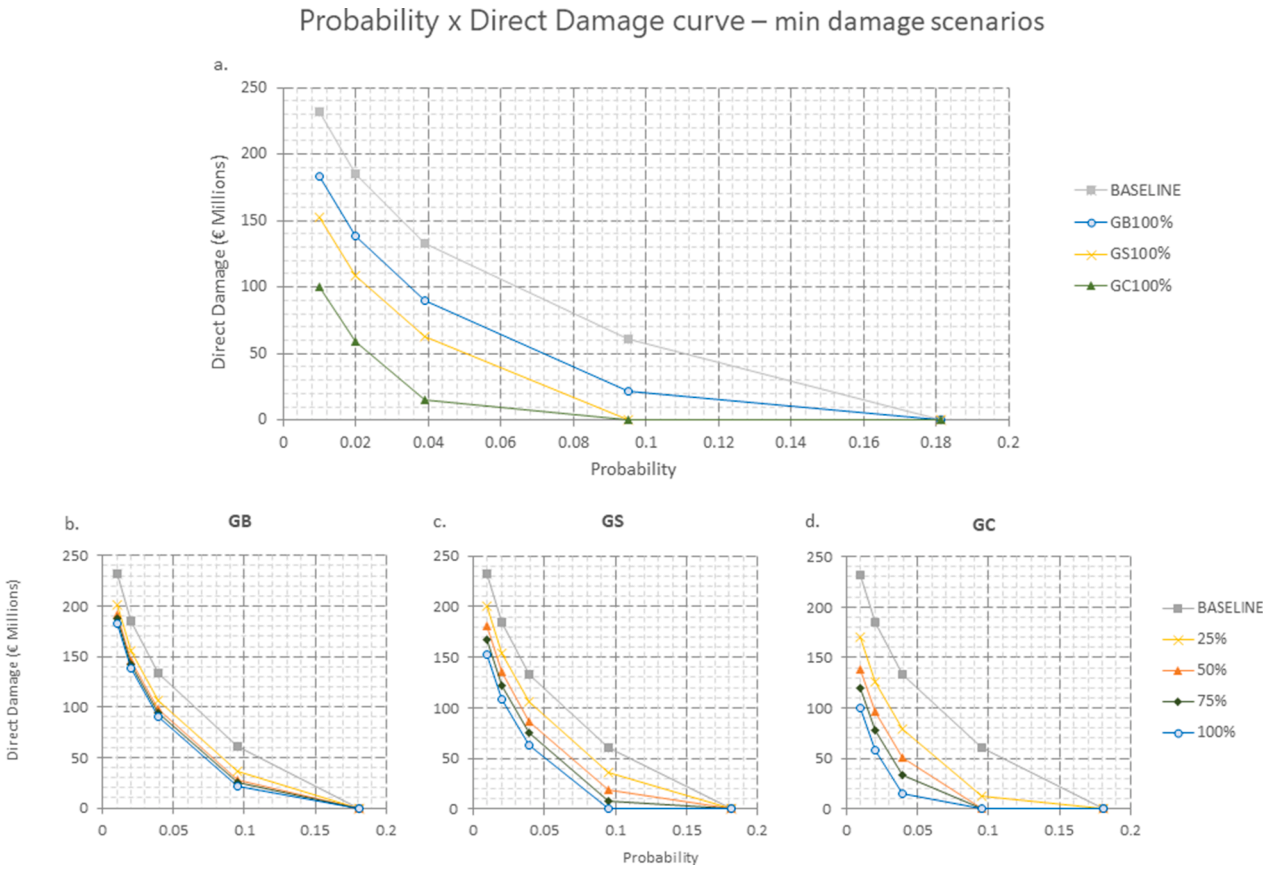

Fig. 7. Expected damage versus probability curves when assuming a maximum drainage capacity corresponding to a precipitation event of RP5. a) comparison of direct damages for 100% of green in all scenarios; b) Estimated direct damages for Green Buildings scenarios; c) Estimated direct damages for Green Spaces scenarios; d) Expected direct damages for Green City scenarios.

Table 3
Summary table of expected annual damage in all scenarios of green conversion when assuming a maximum drainage capacity corresponding to a precipitation event of RP5.

Expected Annual Damage (M€)			
	Green Buildings	Green Spaces	Green City
Baseline	18.56	18.56	18.56
25%	14.11	13.97	9.59
50%	12.60	10.92	6.08
75%	12.08	8.96	4.58
100%	11.39	7.13	2.98

(between 10–65 % and 20–99 % in RP10 and RP25 max. drainage capacity). For people exposed to extreme pluvial floods, Green City scenarios show a reduction of 100 % for lower rain intensities, up to 50 % in RP100 events (around 70 % and 100 % in RP10 and RP25 max. drainage capacity). Percentage reduction ranges from 11 % to around 18 % in Green Buildings scenarios, and from 17 % to 34 % in Green Spaces scenarios (11–25 %, 20–85 % in GB, 12-45 %, 22–80 % in GS for RP10 and RP25 max. drainage capacity respectively). The larger decrease in the population exposed to water depth > 100 cm can be explained by the fact that green areas progressively reduce the water depth in the city, and so that the population living in higher water depth classes tends to move to lower exposure classes, resulting in an overall higher number of exposed people. This is happening again for each rainfall event, with higher impacts in case of low-intermediate rain intensities. Comparing the effects associated with the two minimisation goals, higher reduction can be found in the lower levels of green conversion in the configuration to minimise population exposed and comparable results in the 100 % of potential greening.

The expected annual population exposed confirmed a notable reduction at the increasing of green coverage. At the current conditions, the total EAPE to water depth > 5 cm counts almost 2500 persons, and around 500 persons exposed to extreme class of water depth > 100 cm (1016 and 226 in water depth>5 cm and 240 and 53 in water depth > 100 cm for RP10 and RP25 max drainage capacity respectively). In GC scenarios, the 25 % of additional green coverage contribute to reduce the population exposed of around 40–42 % for both classes of water depth > 5 cm and class >100 cm (see Table 4 and Figs. 9 and 10) (around 40 % and 60–68 % reduction in RP10 and RP25 max. drainage capacity). At the same percentage of conversion, the EAPE is reduced by 18–20 % GS and 28–30 % in GB (20–25 % and 25–30 % in GB, 30–35 % and 45–50 % in GS for RP10 and RP25 max. drainage capacity respectively). Similar results are obtained for the EAPE in the minimization of population exposed (in Annex).

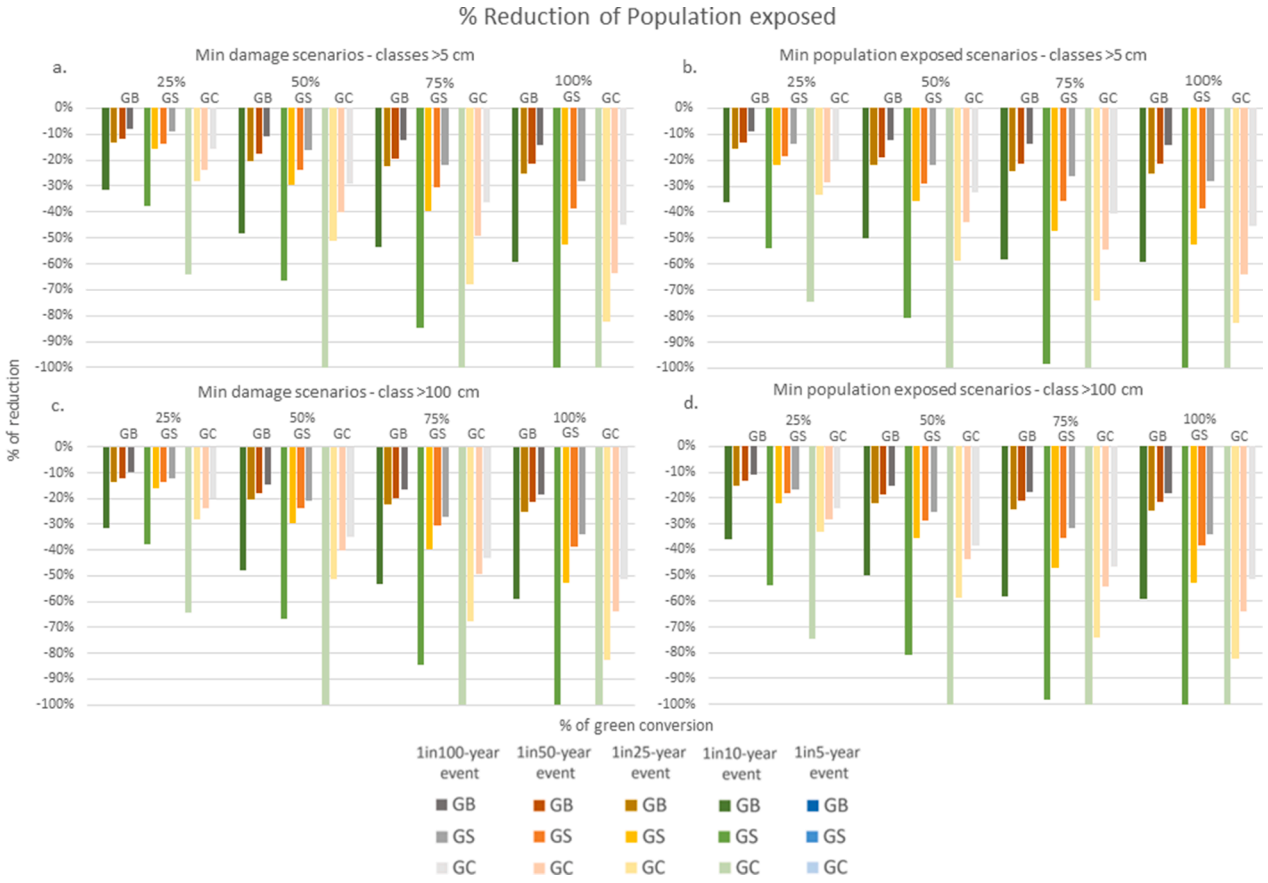

Fig. 8. Percentage reduction of population exposed for each scenario of conversion when assuming a maximum drainage capacity corresponding to a precipitation event of RP5: a-b) reduction of population exposed to classes >5 cm of water depth associated with the minimization of damage scenarios; c-d) reduction of population exposed to extreme class >100 cm of water depth associated with the minimization of population exposed scenarios. X axis represents the percentage of green conversion (25% to 100%) for each scenario of conversion (GB, GS, GC), while y axis reports the percentage reduction of damage to buildings and population exposed.

Table 4
Summary table of expected annual population exposed in all scenarios of green conversion for classes of water depth > 5cm and > 100cm when assuming a maximum drainage capacity corresponding to a precipitation event of RP5.

Expected Annual Population Exposed (nr of people)						
	> 5 cm			>100 cm		
	Green Buildings	Green Spaces	Green City	Green Buildings	Green Spaces	Green City
Baseline	2496	2496	2496	513	513	513
25%	2136	2071	1721	422	393	327
50%	1939	1674	1087	375	306	201
75%	1863	1370	838	360	246	153
100%	1792	1074	623	343	200	103

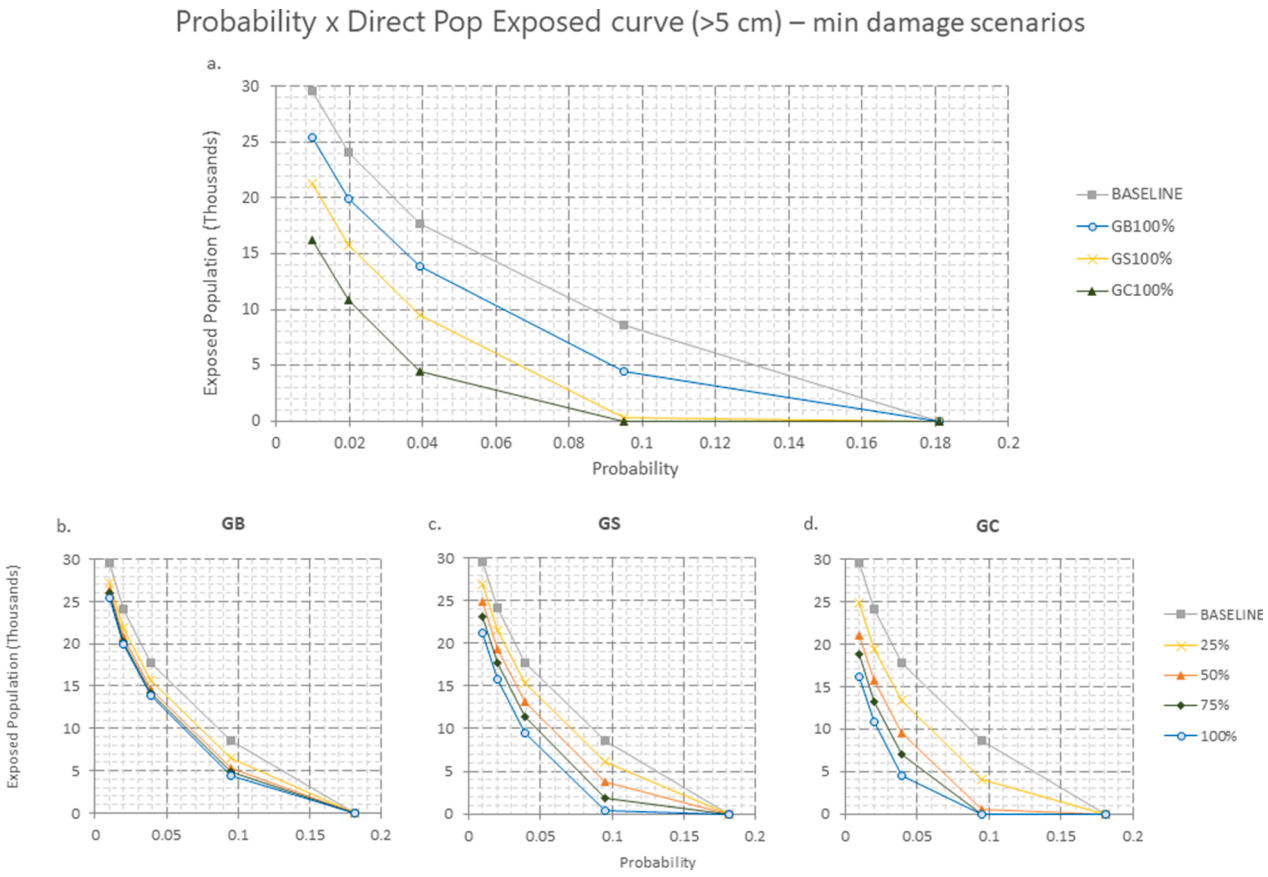

Fig. 9. Expected annual population exposed values versus probability curves for classes of water depth > 5 cm when assuming a maximum drainage capacity corresponding to a precipitation event of RP5. a) comparison of population exposed for 100% of green in all scenarios; b) estimated population exposed for Green Buildings scenarios; c) estimated population exposed for Green Spaces scenarios; d) expected population exposed for Green City scenarios.

4.3.3. Overall assessment

The spatial distribution of damage and population exposed reduction per unit of area is shown in Fig. 11. It reported the 25 % of conversion in the Green City scenarios for RP100 rainfall events, showing the effects associated with the two minimization goals analysed. The highest ranked areas for percentage reduction of impacts are similarly distributed across the city in both rainfall events. Areas with higher reduction of population exposed are located mostly in the north or in the very south of the studied area. Areas with higher reduction potential in terms of direct economic damages are distributed all around the city centre. Clusters of higher economic impacts are recognizable in the north-east, south-east and south-west. In general, the higher ranked areas are mostly concentrated where the surround green coverage is higher. The spatial ranking of areas with the higher reduction potential is not changing with the maximum drainage capacity assumed.

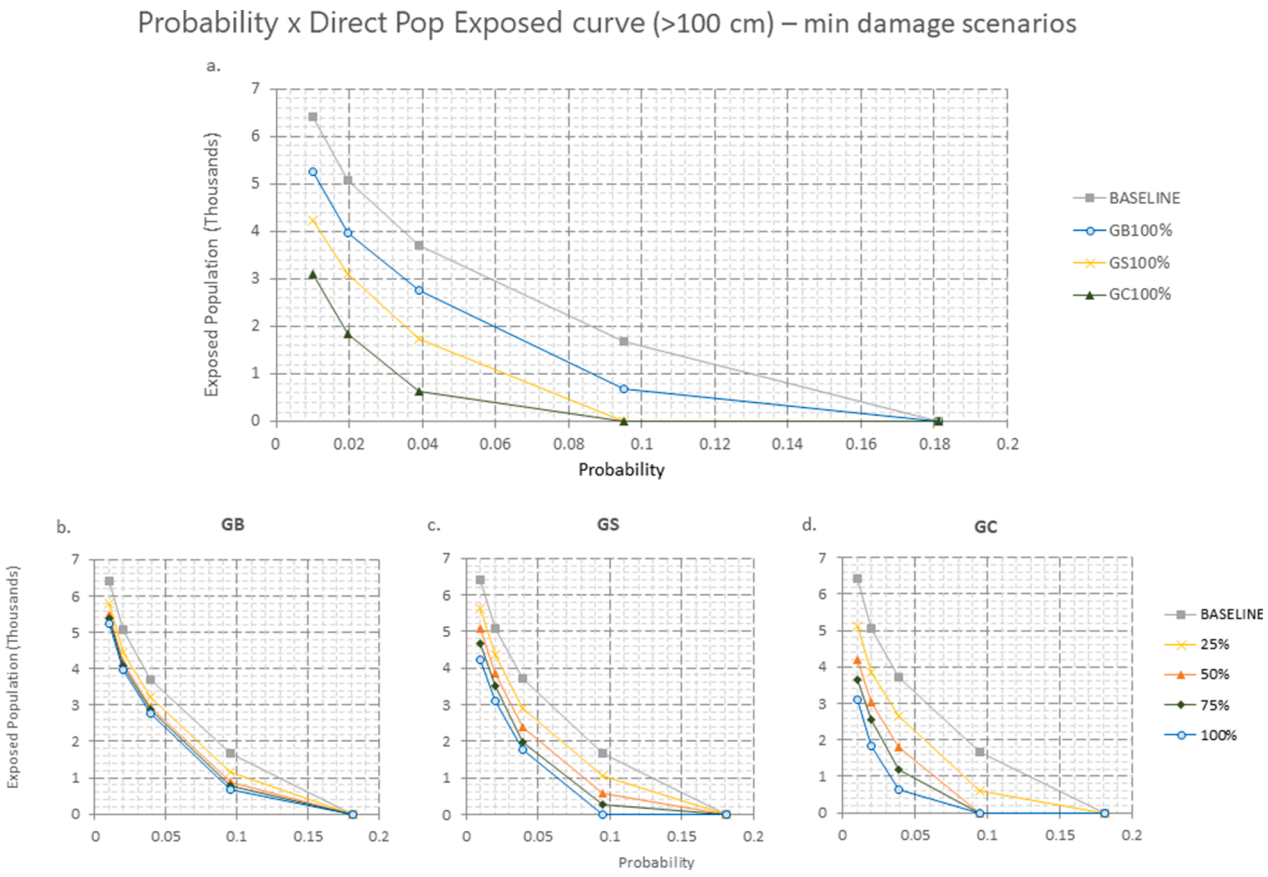

Fig. 10. Expected annual population exposed versus probability curves for class of water depth > 100 cm when assuming a maximum drainage capacity corresponding to a precipitation event of RP5. a) comparison of population exposed for 100% of green in all scenarios; b) estimated population exposed for Green Buildings scenarios; c) estimated population exposed for Green Spaces scenarios; d) estimated population exposed for Green City scenarios.

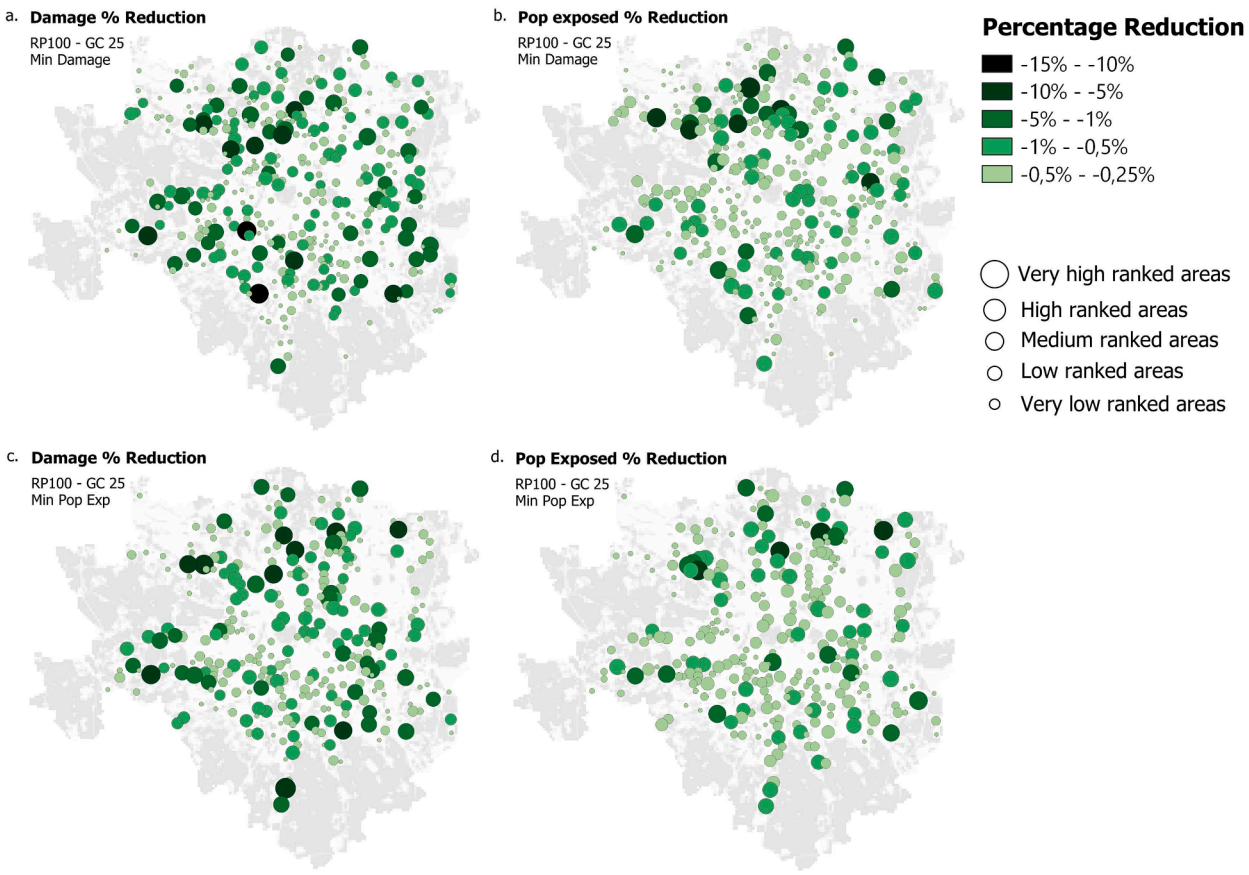

Fig. 11. Spatial representation of damage and population exposed reduction per unit of area in the 25% Green City scenario for a rainfall event RP100: a-b) reduction associated with the minimization of damage scenarios; c-d) reduction associated with the minimization of population exposed scenarios. Population exposed here counts for all classes >5cm.

5. Discussion

The analysis of scenarios identified several options for improving the city's green infrastructure. The scenarios focused on different approaches, as the conversion of buildings, the conversion of open spaces and a combination of both. All scenarios investigated showed positive impacts on pluvial flood mitigation, reducing both direct damages to buildings and population exposed. Even with a lower conversion percentage (25 % of green improvement), green interventions have the potential to halve the pluvial flood damages and decrease the population exposed by 40 %. Generally, all scenarios showed a slightly better response to lower rain intensities, but with significant contribution even in the case of more extreme rainfall events. Flood risk also depends not only on rain intensity but also on soil infiltration capacity, which is a function of soil characteristics and properties that can limit the amount of water retained in and passing by soil layers (Ren et al., 2020). Therefore, higher reduction impacts are linked to larger extent of green coverage and to different types of conversion combined together. Strategies that rely solely on a single approach had a limited effectiveness. In all the cases investigated, Green City scenarios provided larger positive benefits compared to Green Space and Green Building scenarios. This suggests that multiple and diverse interventions, spatially distributed and connected across the space, should be considered to have more benefits. They can include different NBS options or the integration of green and more traditional interventions. Green conversion should be specifically designed according to the context, implementing, for example, urban parks, rain gardens, green roofs and walls, vegetated alleys, or green rail paths. It is often not feasible to completely convert an area to green, therefore NBS should be used in conjunction with the urban drainage system and more engineered solutions, to increase the potential water retention capacity during extreme rainfall events. While Green Building and Green Space scenarios have a lower impact on reducing flood risk, they can still provide valuable insight for the distribution of green interventions throughout the city. The implementation of diverse nature-based interventions, which can be applied differently across the city, can enhance both green connectivity and to the overall effectiveness of flood risk reduction. This is in line with recent reviews and studies, finding that the potential limited effectiveness to cope with extreme pluvial flooding can be compensated by the joint implementation and the use of diverse types of both green and grey solutions across the city, that differently contribute to mitigate flood risk (Huang et al., 2020; Costa et al., 2021; Majidi et al., 2019).

As shown in the Results and Annex sections, the presence of a stormwater drainage system and the associated capacity levels is a main driver of the direct impact estimates. However, the location in which areas can potentially be converted to green areas remains largely unchanged, a result that is potentially attributed to the spatial-consistent assumption of stormwater drainage system capacity. Overall, the determination of flood risk hotspots, the spatial distribution, and the prioritization of areas with a more substantial impact on pluvial flood risk reduction remain largely unaffected by the considered assumptions of different maximum drainage capacity. Furthermore, the diverse scenarios of green conversion exhibit similar behaviour across various assumptions of no damage. In practice, assuming a spatially consistent and flawlessly designed urban stormwater drainage system is per se a source of uncertainty not to be neglected in case the methods proposed in this paper are to be replicated in a real-world context. In spatial terms, overlooking the precise location and specific attributes of urban drainage systems introduces errors that can potentially impact the model's results in determining the locations susceptible to flooding.

Nevertheless, these negative effects are expected to diminish for more severe, less frequent precipitation events as the capacity of stormwater drainage network systems is exceeded.

The administration can prioritize green conversion interventions based on the spatial ranking of areas with higher positive impacts. This can help minimize the economic damages, the population affected or both, depending on the goal pursued. The priority areas are located in the districts characterised also by higher social and material vulnerability, particularly in the north-west (Istat, 2020). This could motivate actions in areas, where the population may have a lower capacity to recover after a disaster, such as those. with lower economic capacity, poorer labour conditions, more fragile social and housing conditions, or a higher proportion of elderly residents. The spatial ranking of priority areas can be, however, subject to the importance or weight of each criterion used. In this case, we limited our analysis to equally weighted criteria to demonstrate the overall application of this approach. However, the study could be further improved by engaging key stakeholders and decision-makers would contribute to better tailor scenarios of green conversion, in accordance with diverse management or development plans. Furthermore, stakeholder's engagement could aid in incorporating a cost-benefit analysis into the assessment. By targeting the analysis on particular green solutions, it would be possible to account for the costs of implementing and maintaining such solutions in relation to the benefits they provide. When developing adaptation strategies, it is essential to have information for designing specific interventions. This information also supports a more in-depth analysis of additional co-benefits, such us improved biodiversity or health-related benefits. However, estimating benefits in economic or monetary terms can be challenging, particularly when considering more ecological and social benefits, hindering the application of cost-benefit analysis.

The approach presented in the study is aimed to provide a quick analysis to obtain an overview of hotspot risk areas, potential distributions and impacts of nature-based interventions. This analysis can guide the development of specific measures through a more detailed investigation. The approach can be adapted to different realities as an investigative tool to support tailored strategies according to city goals. In this perspective, the analysis could be further extended to include additional scenarios of green conversion, alternative greening solutions or different city resilience goals. Further analysis could consider climate change scenarios and related uncertainties, or address different types of hazards, such as heat waves, to support a better understand and quantify urban green benefits also in future and diverse conditions. Nature-based interventions may require time to become fully operational and may also be subject to the impacts of climate change (Calliari et al., 2019). Therefore, this would be particularly relevant to define plans and strategies that take into account changes in the distribution of flood risks, as well as in the effectiveness of solutions over time.

6. Conclusions

The paper proposes an analysis to assess the potential impacts of on urban green infrastructure network on the reduction of pluvial flood risk. The scenarios developed help to prioritise areas of interventions and have an insight of the overall effects to guide decision-makers, urban plans and strategies. However, the design of specific measures and solutions in these areas will require further investigation. This study is also useful for identifying priorities for investments in nature-based solutions and urban ecosystem restoration. Urban green network can be connected to and integrated into a regional ecological network, contributing so to more sustainable interactions between nature and society, that support human, ecosystem and planetary health (IPCC, 2022). Multifunctional urban green infrastructure can contribute to thermal comfort, air quality, carbon sequestration, and multiple health, social and recreational benefits in addition to risk reduction. Robust evidence of damage reduction could support the development of insurance and investments schemes, to help bridge the financing gap for nature-based solutions.

CRediT authorship contribution statement

Andrea Staccione: Conceptualization, Data curation, Formal analysis, Methodology, Visualization, Writing – original draft, Writing – review & editing. **Arthur Hrast Essenfelder:** Conceptualization, Data curation, Formal analysis, Methodology, Visualization, Writing – original draft, Writing – review & editing. **Stefano Bagli:** Conceptualization, Methodology, Software, Writing – review & editing. **Jaroslav Mysiak:** Conceptualization, Funding acquisition, Methodology, Supervision, Writing – review & editing.

Declaration of competing interest

The authors declare that they have no known competing financial interests or personal relationships that could have appeared to influence the work reported in this paper.

Data availability

Data will be made available on request.

Acknowledgements

This research was developed in the context of EFLIP Project (Economic impacts of Flood risk in Lombardy and Innovative risk mitigation Policy), grant agreement n. 2017-0735, and supported by European Union's Horizon 2020 research and innovation programme under grant agreement No 101036599, Project "REACHOUT - Resilience in Europe through Activating City Hubs reaching Out to Users with triple-A climate adaptation Tools".

Supplementary materials

Supplementary material associated with this article can be found, in the online version, at doi:10.1016/j.scs.2024.105288.

References

Andrés-Doménech, I., Perales-Momparler, S., Morales-Torres, A., & Escuder-Bueno, I. (2018). Hydrological performance of green roofs at building and city scales under mediterranean conditions. *Sustainability (Switzerland), 10*, 1–15. https://doi.org/10.3390/su10093105

C40 Cities, Milan: https://www.c40.org/cities/milan/, last access: 9 January 2024.

Calliari, E., Staccione, A., & Mysiak, J. (2019). An assessment framework for climate-proof nature-based solutions. *Science of the Total Environment, 656*. https://doi.org/10.1016/j.scitotenv.2018.11.341

Carrera, L., Standardi, G., Koks, E. E., Feyen, L., Mysiak, J., Aerts, J., and Bosello, F.: Economics of flood risk in Italy under current and future climate., CMCC Research Paper, 2015.

Chang, H., Pallathadka, A., Sauer, J., Grimm, N. B., Zimmerman, R., Cheng, C., Iwaniec, D. M., Kim, Y., Lloyd, R., McPhearson, T., Rosenzweig, B., Troxler, T., Welty, C., Brenner, R., & Herreros-Cantis, P. (2021). Assessment of urban flood vulnerability using the social-ecological-technological systems framework in six US cities. *Sustainable Cities and Society, 68*, Article 102786. https://doi.org/10.1016/j.scs.2021.102786

Cirrincione, L., Marvuglia, A., & Scaccianoce, G. (2021). Assessing the effectiveness of green roofs in enhancing the energy and indoor comfort resilience of urban buildings to climate change: Methodology proposal and application. *Building and Environment, 205*, Article 108198. https://doi.org/10.1016/j.buildenv.2021.108198

CNR-GNDCI: VAPI (Flood Evaluation) Project — Progetto VAPI Sulla Valutazione Delle Piene in Italia, 2001.

Comune di Milano: Tetti Verdi potenziali, 2016.

Comune di Milano: Milano 2030. Piano di Governo del Territorio (PGT) - Allegato 2 del Rapporto Ambientale: Quadro di riferimento territorial e ambientale, 2019a.

Comune di Milano: Piano di Governo del Territorio (PGT) Milano 2030, 2019b.

Comune di Milano: Piano Aria e Clima, 2020.

Costa, S., Peters, R., Martins, R., Postmes, L., Keizer, J. J., & Roebeling, P. (2021). Effectiveness of nature-based solutions on pluvial flood hazard mitigation: The case study of the city of eindhoven (the netherlands). *Resources, 10*. https://doi.org/10.3390/resources10030024

da Silva, L. B. L., Alencar, M. H., & de Almeida, A. T. (2022). A novel spatiotemporal multi-attribute method for assessing flood risks in urban spaces under climate change and demographic scenarios. *Sustainable Cities and Society, 76*, Article 103501. https://doi.org/10.1016/j.scs.2021.103501

Dottori, F., Mentaschi, L., Bianchi, A., Alfieri, L., and Feyen, L.: JRC Technical report. Adapting to rising river flood risk in the EU under climate change JRC PESETA IV project-Task 5, doi:10.2760/14505, 2020.

Du, S., Wang, C., Shen, J., Wen, J., Gao, J., Wu, J., Lin, W., & Xu, H. (2019). Mapping the capacity of concave green land in mitigating urban pluvial floods and its beneficiaries. *Sustainable Cities and Society, 44*, 774–782. https://doi.org/10.1016/j.scs.2018.11.003

EC: COM (2013) 249 final: Green Infrastructure (GI) — Enhancing Europe's Natural Capital, 2013a.

EC: Synthesis document n ° 1 - Intorducing Natural Water Retention Measures: what are NWRM?, 2013b.

EC: Towards an EU Research and Innovation policy agenda for Nature-Based Solutions & Re-Naturing Cities, Brussels, Belgium, 74 pp., doi:10.2777/440514, 2015.

edited by Misiune, I., & Kazys, J. (2022). Accessibility to and fragmentation of urban green infrastructure: Importance for adaptation to climate change. In I. Misiune, D. Depellegrin, & L. Egarter Vigl (Eds.), *Human-Nature Interactions: Exploring Nature's Values Across Landscapes* (pp. 235–246). Cham: Springer International Publishing. https://doi.org/10.1007/978-3-031-01980-7_19. edited by.

EEA: Green Infrastructure and Flood Management: Promoting cost-efficient flood risk reduction via green infrastructure solutions, 155 pp., 2017.

EEA: Nature-based solutions in Europe: Policy, knowledge and practice for climate change adaptation and disaster risk reduction, 159 pp., doi:10.2800/919315, 2021.

EEA: Briefing no. 21/2021: Economic losses and fatalities from weather- and climate-related events in Europe, doi:10.2800/7654, 2022.

EEA. (2018). *Imperviousness density layer*. European Environment Agency. https://land.copernicus.eu/pan-european/high-resolution-layers/imperviousness/status-maps/imperviousness-density-2018?tab=metadata.

Ekmekcioğlu, Ö., Koc, K., & Özger, M. (2022). Towards flood risk mapping based on multi-tiered decision making in a densely urbanized metropolitan city of Istanbul. *Sustainable Cities and Society, 80*, Article 103759. https://doi.org/10.1016/j.scs.2022.103759

Ercolani, G., Chiaradia, E. A., Gandolfi, C., Castelli, F., & Masseroni, D. (2018). Evaluating performances of green roofs for stormwater runoff mitigation in a high flood risk urban catchment. *Journal of Hydrology, 566*, 830–845. https://doi.org/10.1016/j.jhydrol.2018.09.050

Essenfelder, A. H., Bagli, S., Mysiak, J., Pal, J. S., Mercogliano, P., Reder, A., Rianna, G., Mazzoli, P., Broccoli, D., & Luzzi, V. (2022). Probabilistic assessment of pluvial flood risk across 20 european cities: A demonstrator of the Copernicus disaster risk reduction service for pluvial flood risk in urban areas. *Water Economics and Policy*. https://doi.org/10.1142/S2382624X22400070

Ferri, S., Siragusa, A., Sabo, F., Pafi, M., and Halkia, M.: The European Settlement Map 2017 Release, doi:10.2760/41305, 2017.

Fischer, E. M., & Knutti, R. (2016). Observed heavy precipitation increase confirms theory and early models. *Nature Climate Change, 6*, 986–991. https://doi.org/10.1038/nclimate3110

Harris, EC (2010). International buildings costs worldwide. Annual report. May 2010. ECHarris Built Asset Consultancy.

Huang, Y., Tian, Z., Ke, Q., Liu, J., Irannezhad, M., Fan, D., Hou, M., & Sun, L. (2020). Nature-based solutions for urban pluvial flood risk management. *WIREs Water, 7*. https://doi.org/10.1002/wat2.1421

Huizinga, J., De Moel, H. and Szewczyk, W., Global flood depth-damage functions: Methodology and the database with guidelines, EUR 28552 EN, Publications Office of the European Union, Luxembourg, 2017, ISBN 978-92-79-67781-6, doi:10.2760/16510, JRC105688.

IPCC: Summary for policymakers: Managing the risks of extreme events and disasters to advance climate change adaptation. A special report of working groups I and II of the intergovernmental panel on climate change., doi:10.1017/CBO9781139177245, 2012.

IPCC: Climate change 2021: The physical science basis. Summary for policy makers, 2021.

ISTAT: Rapporto Sul Territorio 2020 - Ambiente, Economia E Società, doi:10.1481/Istat.Rapportoterritorio.2020, 2020.

Istat: Le Misure Della Vulnerabilità: Un'Applicazione a Diversi Ambiti Territoriali, 2020.

ISTAT: I cambiamenti climatici: misure statistiche 2020, 2022.

La Rosa, D., & Pappalardo, V. (2020). Planning for spatial equity - A performance based approach for sustainable urban drainage systems. *Sustainable Cities and Society, 53*, Article 101885. https://doi.org/10.1016/j.scs.2019.101885

Lastoria, B., Bussettini, M., Mariani, S., Piva, F., & Braca, G. (2021). *Rapporto sulle condizioni di pericolosità da alluvione in Italia e indicatori di rischio associati.* Roma: ISPRA. edited by.

Laurenti, M. and Bono, L.: Ecosistema Urbano: Rapporto sulle prformance ambientali dellle città 2020, 207, 2020.

Łukaszkiewicz, J., Fortuna-antoszkiewicz, B., Oleszczuk, Ł., and Fialová, J.: The potential of tram networks in the revitalization of the Warsaw landscape, 7–11, 2021.

Majidi, A. N., Vojinovic, Z., Alves, A., Weesakul, S., Sanchez, A., Boogaard, F., & Kluck, J. (2019). Planning nature-based solutions for urban flood reduction and thermal comfort enhancement. *Sustainability (Switzerland), 11*. https://doi.org/10.3390/su11226361

Mitchell, M. G. E., Suarez-Castro, A. F., Martinez-Harms, M., Maron, M., McAlpine, C., Gaston, K. J., Johansen, K., & Rhodes, J. R. (2015). Reframing landscape fragmentation's effects on ecosystem services. *Trends in Ecology & Evolution, 30*, 190–198. https://doi.org/10.1016/J.TREE.2015.01.011

Monteiro, R., Ferreira, J. C., & Antunes, P. (2020). Green infrastructure planning principles: An integrated literature review. *Land, 9*, 1–19. https://doi.org/10.3390/land9120525

Moreno, C., Allam, Z., Chabaud, D., Gall, C., & Pratlong, F. (2021). Introducing the "15-minute city": Sustainability, resilience and place identity in future post-pandemic cities. *Smart Cities, 4*, 93–111. https://doi.org/10.3390/smartcities4010006

Myhre, G., Alterskjær, K., Stjern, C. W., Hodnebrog, Marelle, L., Samset, B. H., Sillmann, J., Schaller, N., Fischer, E., Schulz, M., & Stohl, A. (2019). Frequency of extreme precipitation increases extensively with event rareness under global warming. *Scientific Reports, 9*, 1–10. https://doi.org/10.1038/s41598-019-52277-4

Mysiak, J., Daniell, J., & Vanneuville, W. (2022). Economic losses from weather and climate-related events in Europe, technical report of the European topic centre on climate change impacts. *Vulnerability and Ad-aptation (ETC-CA)*. Copenhagen, Denmark, Copenhagen (Denmark): European Environment Agency.

Olsen, A. S., Zhou, Q., Linde, J. J., & Arnbjerg-Nielsen, K. (2015). Comparing methods of calculating expected annual damage in urban pluvial flood risk assessments. *Water (Switzerland), 7*, 255–270. https://doi.org/10.3390/w7010255

OSM: OpenStreetMaps, 2021.

Pamukcu-Albers, P., Ugolini, F., La Rosa, D., Grădinaru, S. R., Azevedo, J. C., & Wu, J. (2021). Building green infrastructure to enhance urban resilience to climate change and pandemics. *Landscape Ecology, 36*, 665–673. https://doi.org/10.1007/s10980-021-01212-y

Panagos, P (2006). The European soil database.GEO. *Connexion, 5*(7), 32–33.

Pascual-Hortal, L., & Saura, S. (2006). Comparison and development of new graph-based landscape connectivity indices: towards the priorization of habitat patches and corridors for conservation. *Landscape Ecology, 21*, 959–967. https://doi.org/10.1007/s10980-006-0013-z

Piyumi, M. M. M., Abenayake, C., Jayasinghe, A., & Wijegunarathna, E. (2021). Urban flood modeling application: Assess the effectiveness of building regulation in coping with urban flooding under precipitation uncertainty. *Sustainable Cities and Society, 75*, Article 103294. https://doi.org/10.1016/j.scs.2021.103294

IPCC: Climate change 2022: Impacts, Adaptation, and Vulnerability. Contribution of Working Group II to the sixth assessment report of the intergovernmental panel on climate change H.-O. Pörtner, D.C. Roberts, M. Tignor, E.S. Poloczanska, K. Mintenbeck, A. Aleg, 2022.

Regione Lombardia: Consultazione e distribuzione delle foto aeree e dei rilievi Lidar., 2022.

Ren, X., Hong, N., Li, L., Kang, J., & Li, J. (2020). Effect of infiltration rate changes in urban soils on stormwater runoff process. *Geoderma, 363*, Article 114158. https://doi.org/10.1016/j.geoderma.2019.114158

Resilient Cities Network, Milan: https://resilientcitiesnetwork.org/milan/, last access: 9 January 2024.

Samela, C., Persiano, S., Bagli, S., Luzzi, V., Mazzoli, P., Humer, G., Reithofer, A., Essenfelder, A., Amadio, M., Mysiak, J., & Castellarin, A. (2020). Safer_RAIN: A DEM-based hierarchical filling-&-spilling algorithm for pluvial flood hazard assessment and mapping across large urban areas. *Water, 12*, 1514. https://doi.org/10.3390/w12061514

Saura, S., & Rubio, L. (2010). A common currency for the different ways in which patches and links can contribute to habitat availability and connectivity in the landscape. *Ecography, 33*, 523–537. https://doi.org/10.1111/j.1600-0587.2009.05760.x

Schiavina, M., Freire, S., and MacManus, K.: GHS population grid multitemporal (1975, 1990, 2000, 2015) R2019A, doi:10.2905/0C6B9751-A71F-4062-830B-43C9F432370F, 2019.

Sharifi, A. (2021). Co-benefits and synergies between urban climate change mitigation and adaptation measures: A literature review. *Science of the Total Environment, 750*. https://doi.org/10.1016/j.scitotenv.2020.141642

SISI: Popolazione residente Comune di Milano 2021, 2021.

Skougaard Kaspersen, P., Høegh Ravn, N., Arnbjerg-Nielsen, K., Madsen, H., & Drews, M. (2017). Comparison of the impacts of urban development and climate change on exposing European cities to pluvial flooding. *Hydrology and Earth System Sciences, 21*, 4131–4147. https://doi.org/10.5194/hess-21-4131-2017

Soille, P., & Vogt, P. (2009). Morphological segmentation of binary patterns. *Pattern Recognition Letters, 30*, 456–459. https://doi.org/10.1016/J.PATREC.2008.10.015

Spano, D., Armiento, M., Aslam, M.F., Bacciu, V., Bigano, A., Bosello, F., Breil, M., Buonocore, M., Butenschön, M., Cadau, M., Cogo, E., Colell, F.P., Costa Saura, J.M., Dasgupta, S., Cian, E.D., Debolini, M., Didevarasl, A., Ellena, M., Galluccio, G., Harris, R., Johnson, K., Libert, A., Lo Cascio, M., Lovato, T., Marras, S., Masina, S., Mercogliano, P., Mereu, V., Mysiak, J., Noce, S., Papa, C., Phelan, A.S., Pregagnoli, C., Reder, A., Ribotta, C., Sano, M., Santini, A., Santini, M., Sartori, N., Sini, E., Sirca, C., Tharmananthan, R., Torresan, S., and Trabucco, A.: G20 Climate Risk Atlas Impacts, policy and economics in the G20, doi:10.25424/cmcc/g20_climaterisk, 2021b.

Spano, D., Mereu, V., Bacciu, V., Barbato, G., Buonocore, M., Casartelli, V., Ellena, M., Lamesso, E., Ledda, A., Marras, S., Mercogliano, P., Monteleone, L., Mysiak, J., Padulano, R., Raffa, M., Ruiu, M.G.G., Serra, V., and Villani, V.: Analisi del rischio: i cambiamenti climatici in sei città italiane, doi:10.25424/cmcc/analisi_del_rischio_2021, 2021a.

edited by Staccione, A., Candiago, S., & Mysiak, J. (2022a). A network approach to green infrastructure: How to enhance ecosystem services provision? In I. Misiune, D. Depellegrin, & L. Egarter Vigl (Eds.), *Human-Nature Interactions: Exploring Nature's Values Across Landscapes* (pp. 51–60). Cham: Springer International Publishing. https://doi.org/10.1007/978-3-031-01980-7_5. edited by.

Staccione, A., Candiago, S., & Mysiak, J. (2022b). Mapping a Green Infrastructure Network: A framework for spatial connectivity applied in Northern Italy.

Environmental Science & Policy, 131, 57–67. https://doi.org/10.1016/J.ENVSCI.2022.01.017

Sudmeier-Rieux, K., Arce-Mojica, T., Boehmer, H. J., Doswald, N., Emerton, L., Friess, D. A., Galvin, S., Hagenlocher, M., James, H., Laban, P., Lacambra, C., Lange, W., McAdoo, B. G., Moos, C., Mysiak, J., Narvaez, L., Nehren, U., Peduzzi, P., Renaud, F. G., Sandholz, S., Schreyers, L., Sebesvari, Z., Tom, T., Triyanti, A., Van Eijk, P., Van Staveren, M., Vicarelli, M., & Walz, Y. (2021). Scientific evidence for ecosystem-based disaster risk reduction. *Nature Sustainability, 4*, 803–810. https://doi.org/10.1038/s41893-021-00732-4

UNEP and UN-Habitat: Global Environment for Cities-GEO for Cities: Towards Green and Just Cities, 2021.

Vogt, P., Ferrari, J. R., Lookingbill, T. R., Gardner, R. H., Riitters, K. H., & Ostapowicz, K. (2009). Mapping functional connectivity. *Ecological Indicators, 9*, 64–71. https://doi.org/10.1016/j.ecolind.2008.01.011

Zanchini, E., Nanni, G., and Minutolo, A.: Il Clima è già cambiato. Rapporto dell'osservatorio di Legambiente Città Clima, 2020.